RESEARCH ARTICLE

Mechanism of persistent hyperalgesia in neuropathic pain caused by chronic constriction injury

Qin-Yi Chen[1, 2, 3, #], Chao-Yang Tan[2, 3, #], Yang Wang[2, 3], Ke-Tao Ma[2, 3], Li Li[2, 3, *], Jun-Qiang Si[2, 3, 4, *]

1 Department of Anesthesiology, First Affiliated Hospital of Shihezi University, Shihezi, Xinjiang Uygur Autonomous Region, China
2 Department of Physiology, Medical College of Shihezi University, Shihezi, Xinjiang Uygur Autonomous Region, China
3 Key Laboratory of Xinjiang Endemic and Ethnic Disease, Shihezi University School of Medicine, Shihezi, Xinjiang Uygur Autonomous Region, China
4 Department of Neurobiology, Tongji Medical College, Huazhong University of Science and Technology, Wuhan, Hubei Province, China

Funding: *This study was supported by the National Natural Science Foundation of China, No. 30160026 (to JQS); the High Level Talent Research Project of Shihezi University of China, No. RCSX201705 (to YW).*

Graphical Abstract

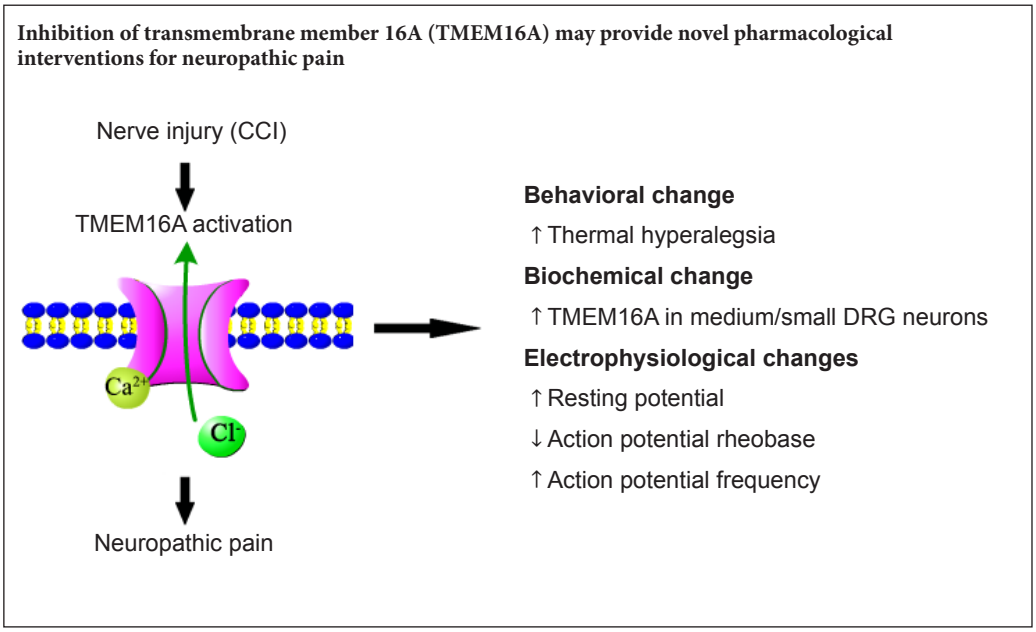

Correspondence to:
Jun-Qiang Si, PhD, sijunqiang@shzu.edu.cn;
Li Li, PhD, lily7588@163.com.

#These authors contributed equally to this paper.

orcid:
0000-0001-6704-2115 (Jun-Qiang Si)
0000-0001-8591-0676 (Li Li)

doi: *10.4103/1673-5374.250631*

Received: *August 10, 2018*
Accepted: *November 11, 2018*

Abstract

Transmembrane member 16A (TMEM16A) is involved in many physiological functions, such as epithelial secretion, sensory conduction, nociception, control of neuronal excitability, and regulation of smooth muscle contraction, and may be important in peripheral pain transmission. To explore the role of TMEM16A in the persistent hyperalgesia that results from chronic constriction injury-induced neuropathic pain, a rat model of the condition was established by ligating the left sciatic nerve. A TMEM16A selective antagonist (10 μg T16Ainh-A01) was intrathecally injected at L5–6. For measurement of thermal hyperalgesia, the drug was administered once at 14 days and thermal withdrawal latency was recorded with an analgesia meter. For measurement of other indexes, the drug was administered at 12 days, once every 6 hours, totally five times. The measurements were performed at 14 days. Western blot assay was conducted to analyze TMEM16A expression in the L4–6 dorsal root ganglion. Immunofluorescence staining was used to detect the immunoreactivity of TMEM16A in the L4–6 dorsal root ganglion on the injured side. Patch clamp was used to detect electrophysiological changes in the neurons in the L4–6 dorsal root ganglion. Our results demonstrated that thermal withdrawal latency was shortened in the model rats compared with control rats. Additionally, TMEM16A expression and the number of TMEM16A positive cells in the L4–6 dorsal root ganglion were higher in the model rats, which induced excitation of the neurons in the L4–6 dorsal root ganglion. These findings were inhibited by T16Ainh-A01 and confirm that TMEM16A plays a key role in persistent chronic constriction injury-induced hyperalgesia. Thus, inhibiting TMEM16A might be a novel pharmacological intervention for neuropathic pain. All experimental protocols were approved by the Animal Ethics Committee at the First Affiliated Hospital of Shihezi University School of Medicine, China (approval No. A2017-170-01) on February 27, 2017.

Key Words: *nerve regeneration; TMEM16A; calcium-activated chloride channels; T16Ainh-A01; neuropathic pain; dorsal root ganglia; hyperalgesia; action potential; rheobase; chronic constriction injury; peripheral nerve injury; neural regeneration*

Chinese Library Classification No. *R453; R363; R741*

Introduction

In 2008, the Neuropathic Pain Special Interest Group (NeuPSIG) of the International Association for the Study of Pain (IASP) updated the definition of neuropathic pain: "neuropathic pain is defined as pain caused by a lesion or disease of the somatosensory system." The NeuPSIG reported that the prevalence of neuropathic pain was from 3.3% to 8.2% (Haanpää et al., 2011). Another study from Europe showed that the prevalence of neuropathic pain in the general population was as high as 8.0% (Tölle, 2010). Based on these data, there are approximately 110 million patients with neuropathic pain in China (Expert group of neuropathological pain diagnosis and treatment, 2013). Although there is no systematic data on the quality of life of patients with neuropathic pain in China, the impact of neuropathic pain on quality of life is obvious. The factors involved in the formation and maintenance of neuropathic pain are extremely complex. Clinical therapeutic drugs have limited efficacy, and many patients must endure long-term side effects of drugs. The development of safe and effective therapeutic drugs requires in-depth study of the pathogenesis of neuropathic pain.

Studies have shown that many cation channels play an important role in the development of neuropathic pain (Xiao et al., 2016; Yang et al., 2018; Yoon et al., 2018), but the role of anion channels remains unclear. Calcium-activated chloride channels (CaCCs) are anion channels that have Ca^{2+}-concentration dependence and use Ca^{2+} as the second messenger. CaCCs are expressed in neurons of the spinal cord, dorsal root ganglion (DRG), and autonomic system. In 2008, transmembrane member 16A (TMEM16A) was determined to be the primary functional molecule in CaCCs (Caputo et al., 2008; Schroeder et al., 2008; Yang et al., 2008). TMEM16A is a class of transmembrane proteins involved in a variety of physiological functions, including epithelial secretion, sensory transduction, nociception, control of neuronal excitability control, and regulation of smooth muscle contraction (Lee et al., 2014; Ruppersburg and Hartzell, 2014; Deba and Bessac, 2015; Wang et al., 2016; Kang et al., 2017). It has been shown that CaCC currents are increased after nerve injury (Boudes et al., 2009). CaCCs, especially their TMEM16A component, can increase the excitability of DRG neurons under inflammatory conditions, exacerbating formalin-mediated inflammatory pain (García et al., 2014; Lee et al., 2014). CaCCs are activated by increased intracellular Ca^{2+} concentration that leads to chloride efflux (Wu et al., 2014; Yamamura et al., 2018). Thus, CaCCs might promote depolarization of nociceptive neurons and be a key factor in the generation of action potentials.

Chronic constriction injury (CCI) was selected as a neuropathic pain model in this experiment. This study assessed the impact of TMEM16A in chronic nociception and long-lasting evoked secondary thermal hyperalgesia elicited by CCI. Furthermore, this study determined the relationship between the expression of TMEM16A and the changes in the excitability of rat DRG.

Material and Methods

Animals

One hundred and fourteen adult male specific-pathogen-free Sprague-Dawley rats weighing 180–200 g and aged 8–12 weeks were purchased from Experimental Animal Center of Xinjiang Medical University, Urumqi, China (certificate No. SCXK (Xin) 2003-0001). All rats were raised in temperature- and humidity-controlled (22°C, 50%) conditions on a 12-hour light/dark cycle, with free access to clean water and food. All experiments followed the Guidelines on Ethical Standards for Investigation of Experimental Pain in Animals (Zimmermann, 1983). All experimental protocols were approved by the Animal Ethics Committee at the First Affiliated Hospital of Shihezi University School of Medicine, China (approval No. A2017-170-01) on February 27, 2017. All procedures minimized the suffering and the number of animals needed for statistical analysis.

Experimental design

Rats were randomly divided into a sham-operated control group (sham group; $n = 6$) and a CCI group ($n = 12$). The thermal withdrawal latency of the rats was measured 1 day before surgery, and 1, 3, 5, 7, 10 and 14 days after surgery. According to the time after CCI, CCI rats were further divided into CCI-7-day and CCI-14-day groups. The sham group, CCI-7-day group, and CCI-14-day group were euthanized and ipsilateral L4–6 DRGs were then harvested to evaluate TMEM16A expression *via* western blot assay. An additional 96 male Sprague-Dawley rats were randomly divided into four groups ($n = 24$ each) after intrathecal catheter implantation: sham group (sham surgery + normal saline), CCI + normal saline (NS) group, CCI + dimethyl sulfoxide (DMSO) group, and CCI + T16Ainh-A01 group. Fourteen days after CCI or sham surgery, rats received an intrathecal injection of vehicle (normal saline or 30% DMSO) or selective TMEM16A inhibitor (T16Ainh-A01) 5 minutes before evaluation of thermal hyperalgesia. The antihyperalgesic effects were evaluated during the following 8 hours. Then, to determine the effect of T16Ainh-A01 on TMEM16A protein expression and DRG excitability, T16Ainh-A01 (10 μg) was intrathecally administered every 6 hours five times starting 12 days after injury. DRG samples were obtained 14 days after surgery, and western blot assays, immunofluorescence analysis, and electrophysiological recordings were conducted (**Figure 1**).

Construction of CCI models

For the construction of the neuropathic pain model, chronic constriction of the sciatic nerve was performed as previously described by Bennett and Xie (1988). Sprague-Dawley rats were intraperitoneally anesthetized with 50 mg/kg of 1% pentobarbital sodium. The left sciatic nerve was exposed and loosely ligated by 4-0 surgical catgut at four ligature points that were approximately 1 mm apart. The ligatures did not affect blood supply of the epicardium. The incision was sutured in layers. In sham-operated rats, the left sciatic nerve was exposed but not ligated. CCI-operated rats exhibiting

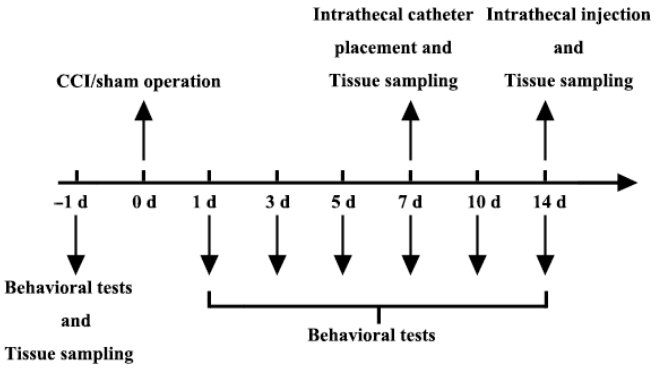

Figure 1 Illustration of the experimental design.
The protocol for exploring dynamic alterations of thermal hyperalgesia, the expression of TMEM16A, and dorsal root ganglion excitability in CCI-induced neuropathic pain. CCI: Chronic constriction injury.

no thermal hyperalgesia at 7 days post-surgery were excluded from the study.

Drug intervention

Intrathecal catheters were implanted were as detailed in a previous study (Pogatzki et al., 2000). Briefly, 7 days following surgery, intraperitoneal anesthesia was induced with 50 mg/kg of 1% pentobarbital sodium, and a 2-cm longitudinal incision was made over the L_{5-6} vertebrae. A polyethylene catheter (PE-10) was pushed through the intervertebral space until a clear cerebrospinal fluid flow was observed, and then gently moved up 2 cm. The other end of the catheter was fixed in the neck area of the rat. Proper intrathecal placement was confirmed by bilateral hind-limb paralysis after injection of 2% lidocaine. T16Ainh-A01 (TMEM16A inhibitor, Cat. No. SML0493; Sigma-Aldrich, St. Louis, MO, USA) was dissolved in 30% DMSO and injected through the catheter.

Evaluation of thermal hyperalgesia

Thermal hyperalgesia was assessed according to a previous protocol (Wang et al., 2017). The thermal withdrawal latency in response to radiant heat stimulation was measured with an analgesia meter (Ugo Basile, Stoelting, IL, USA). The animals were placed in the chamber and allowed to acclimatize for 30 minutes before testing. A radiant heat source was focused under the glass floor beneath the hind paws. Thermal stimulus intensity was adjusted to obtain a baseline thermal withdrawal latency of approximately 20 seconds. The digital timer automatically recorded the duration between stimulus initiation and thermal withdrawal latency. A 30-second cutoff time was used to prevent tissue damage. Each rat was tested every 5 minutes and the average of three trials was used as the thermal withdrawal latency.

Western blot assay

According to a previously reported protocol (Zhang et al., 2018), the L4–6 spinal column was removed after the rats were euthanized. After the spinal cord was removed from the inside of the left spinal canal, the DRGs and its associated nerve roots in the intervertebral foramen were extracted one by one. The nerve roots connected to the DRGs were carefully cut off with fine tweezers and scissors. Protein was extracted from the DRGs of each rat group and protein concentrations were determined using a bicinchoninic acid assay. The protein sample (30 μg) was subjected to sodium dodecyl sulfate polyacrylamide gel electrophoresis (10%) and transferred to a polyvinylidene difluoride membrane (Millipore, Billerica, MA, USA). The membrane was blocked with 5% skim milk at room temperature for approximately 2 hours and then incubated with primary antibody, including rabbit anti-TMEM16A (1:1000, ab53212; Abcam, Cambridge, MA, USA) and mouse anti-beta-actin (1:1000; Santa Cruz Biotechnology, Santa Cruz, CA, USA) overnight at 4°C. After incubating with the respective horseradish peroxidase-conjugated secondary antibody (anti-rabbit or anti-mouse, 1:20,000; Santa Cruz Biotechnology) for 2 hours at room temperature, staining was visualized using enhanced chemiluminescence (GE Healthcare, Chicago, IL, USA). Band intensities were quantified by Image-Pro Plus 6.0 software (Media Cybernetics, Rockville, MD, USA).

Immunofluorescence

According to a previous study (Zhang et al., 2018), rats were anesthetized with 1% pentobarbital sodium (cat. No. P3761, 50 mg/kg, intraperitoneally; Sigma-Aldrich) and perfused through the aorta with 0.9% normal saline. The L4–6 DRG on the surgical side was removed and fixed in 4% paraformaldehyde overnight, followed by dehydration in 20% or 30% sucrose in phosphate buffer at 4°C. The tissue was cut into 5-μm thick sections in a cryostat (Leica CM1950, Nussloch, Germany). The sections were blocked with 5% bovine serum albumin for 1 hour in a 37°C incubator (303-0S; Beijing Ever Bright Medical Treatment Instrument Co., Ltd., Beijing, China) then washed with PBS and incubated with primary antibody (rabbit anti-TMEM16A polyclonal antibody; 1:100, ab53212, Abcam) overnight at 4°C. After washing with PBS, the sections were incubated with the secondary antibody (FITC-conjugated anti-rabbit secondary antibody; 1:100; Santa Cruz Biotechnology) for 1 hour at 37°C. Sections were observed at 200× using a confocal laser scanning microscope (LSM710; Carl Zeiss AG, Oberkochen, Germany). Morphologically, DRG neurons can be divided into large-sized neurons (> 40 μm) and medium/small neurons (< 40 μm) according to their diameters. Optical density measurements and data analysis of TMEM16A positive cells for the two types of DRG neurons were performed using Image-Pro Plus 6.0 software (Media Cybernetics).

Electrophysiological recording

Rats were intraperitoneally anesthetized with 50 mg/kg of 1% pentobarbital sodium. L4–6 DRGs were harvested for electrophysiological recording after continuous intrathecal injection. According to previously described methods (Wang et al., 2017), the whole DRGs were placed into an artificial extracellular fluid maintained at 4°C, supplemented

with 150 mM NaCl, 5.0 mM KCl, 1.0 mM $MgCl_2$, 10 mM hydroxyethyl piperazine ethanesulfonic acid, 10 mM D-glucose, 20 mM sucrose, and 3.32 mM $CaCl_2$. The DRGs were pumped repeatedly using a plastic dropper with digestive solution containing 0.24 mg/mL type-III trypsin (Sigma) and 0.6 mg/mL type-A collagenase (Sigma) for 2–4 minutes at 37°C. After digestion, the cell suspension was dropped into a specific cell culture dish and the cells were allowed to adhere to the wall. Oxygen-saturated extracellular fluid was added after the cells were fully confluent.

For electrophysiological recordings, a 100-fold microscope (Nikon Eclipse Ti, Tokyo, Japan) was used to select DRG cells with smooth membrane surfaces and good translucency for experiments. Subsequently, cells were given slope stimulation (−120 mV to 60 mV, 1000 ms). In current-clamp mode, the cells were given a series of step stimulations to record the action potential. The recorded signal was amplified by a MultiClamp 700B amplifier (Molecular Devices, LLC, Sunnyvale, CA, USA), filtered at 10 kHz, and converted by an Axon Digidata 1550A D/A converter (Molecular Devices, LLC) at a sampling frequency of 10 to 20 kHz.

Statistical analysis

All data are expressed as the mean ± SEM and were analyzed using SPSS 16.0 software (SPSS Inc., Chicago, IL, USA). Statistical differences between the two groups were analyzed by Student's *t* test. One-way analysis of variance followed by the Student-Newman-Keuls test was used to compare differences between more than two groups. A P value < 0.05 was considered statistically significant.

Results

CCI-induced thermal hypersensitivity

Compared with sham-operated rats, CCI decreased withdrawal latency to thermal stimulation. These changes began 1 day after CCI and dropped to the lowest point at 7 days. This downward trend lasted at least 14 days (n = 6, P < 0.001; **Figure 2**). These data indicate that CCI model was successfully established.

TMEM16A expression increases in the DRG after CCI

Western blot assay was used to determine TMEM16A protein expression in sham, CCI-7-day, and CCI-14-day groups. TMEM16A protein level in CCI-7-day rats (n = 6) was higher (P < 0.01) than in the sham-operated group (n = 6), and the difference was even higher for the CCI-14-day rats (n = 6, P < 0.001; **Figure 3**).

T16Ainh-A01 effects on hyperalgesia in CCI rats

Withdrawal latency was significantly shorter in the CCI rats than in the sham-operated rats. The baseline thermal withdrawal latency did not significantly differ between NS and DMSO treated-CCI rats (n = 6; P > 0.05). However, 1 hour after intrathecal administration of T16Ainh-A01 (10 μg) at 14 days post CCI, thermal withdrawal latency of the ipsilateral hind-paw immediately increased, reaching a peak 2 hours after injection. Overall, an obvious antihyperalgesic effect lasted at least 5 hours (n = 6, P < 0.001; **Figure 4**). The inhibitory effect was weakened after the sixth hour, but the difference relative to DMSO-treated CCI rats remained statistically significant (n = 6, P < 0.05; **Figure 4**).

Intrathecal injection of T16Ainh-A01 reduces CCI-induced rise in TMEM16A expression

To ensure the effect of T16Ainh-A01 in decreasing TMEM16A protein expression, DRG neurons were collected from the sham, CCI + NS, CCI + DMSO, and CCI + T16Ainh-A01 groups and the expression of TMEM16A was analyzed. As reported above, TMEM16A expression at 14 days was higher in the CCI group than in the sham-operated group (n = 6, P < 0.001). Intrathecal administration of T16Ainh-A01 reduced CCI-induced TMEM16A protein elevation compared with what was observed in the CCI + DMSO group (n = 6, P < 0.05). This significant difference was not seen between CCI + NS and CCI + DMSO groups (n = 6, P > 0.05; **Figure 5**).

Immunofluorescence analysis showed that trend in TMEM16A fluorescence intensity in both large and medium/small-sized DRG neurons was consistent with the results of the western blot assay. Specifically, TMEM16A expression increased after CCI and decreased after using the inhibitor. Moreover, in four groups, the fluctuation in TMEM16A fluorescence intensity for medium/small-sized neurons was more obvious than that for large neurons. In each group, TMEM16A fluorescence intensity in medium/small-sized neurons was markedly higher than that in large neurons. Additionally, the results confirmed that TMEM16A was primarily expressed in the cytoplasm and membranes of DRG neurons (**Figure 6**).

Inhibition of CCI-induced hyperexcitable state of DRG neurons by T16Ainh-A01, a selective antagonist of TMEM16A

Figure 7A shows an example current patch-clamp recording of DRG neurons in which the firing rate was significantly increased in the CCI + NS and CCI + DMSO groups compared with the sham group. The average number of action potentials produced in the CCI + NS and CCI + DMSO groups was significantly higher than that produced in the sham group (n = 6, P < 0.001; **Figure 7D**). In the CCI + NS and CCI + DMSO groups, the resting potential was slightly elevated and the rheobase of action potentials was significantly reduced compared with the sham group (n = 6, P < 0.001; **Figure 7B** and **C**).

To test the role of TMEM16A in mediating the change in excitability of DRG neurons, we tested the effects of intrathecal injection of T16Ainh-A01 on CCI rats. Intrathecal injection of T16Ainh-A01 resulted in recovered resting potential, reversed the lowered rheobase value, and inhibited the firing rate (**Figure 7B–D**). Meanwhile, there was no differences in resting potential, action potential rheobase, or action potential frequency between CCI + DMSO and CCI + NS groups (n = 6, P > 0.05; **Figure 7**).

Discussion

Neuropathic pain can be induced by peripheral nerve injury (Campbell and Meyer, 2006; Deng et al., 2017; Olukman et al., 2018). Its main features are hyperalgesia, spontaneous pain, and abnormal pain (Jiang et al., 2013). Persistent abnormal discharge of neurons in the injured area and DRG after peripheral nerve injury cause sensitization of the spinal cord, which in turn leads to the development of neuropathic pain symptoms (Li et al., 2018). Change in ion channels is the main reason that abnormal discharge develops, thus the study of ion channels has been a hot topic in pain research.

CaCCs mainly include three families: Bestrophin, Tweenty, and TMEM16. TMEM16A in the TMEM16 family is also called ANO (anoctamin) 1 and is an important CaCC component (Caputo et al., 2008; Schroeder et al., 2008; Yang et al., 2008). TMEM16A was activated by high temperatures above 44°C and highly co-localized with the heat sensor TRPV1 (Cho et al., 2012). TMEM16A is widely expressed in small DRG neurons (Cho et al., 2012). Here, our immunofluorescence results indicated that TMEM16A expression was significantly higher in medium/small DRG neurons than in large DRG neurons. Small DRG neurons are mainly involved in nociceptive regulation, suggesting that TMEM16A plays an important role in this process. Thus, the purpose of this study was to assess the participation of TMEM16A in neuropathic pain induced by CCI in rats.

The CCI model is a neuropathic pain model that simulates peripheral nerve injury. Postoperatively, there were obvious and stable symptoms and signs similar to clinical neuropathic pain, such as spontaneous pain, thermal hyperalgesia, and mechanical allodynia. We found that the thermal withdrawal latency of rats on the first day after CCI began to decrease and thermal hyperalgesia existed for at least 2 weeks. Western blot assay showed that TMEM16A expression in DRG neurons gradually increased after CCI. It was clear that the dynamic time course of TMEM16A expression was consistent with the development and maintenance of heat hyperalgesia in CCI rats, suggesting a possible mechanistic link between TMEM16A upregulation and CCI-induced neuropathic pain. A single intrathecal injection of T16Ainh-A01, a selective TMEM16A inhibitor, transiently relieved the neuropathic pain in CCI rats. Furthermore, T16Ainh-A01 blockade increased CCI-induced TMEM16A expression. Our data agreed with previous studies indicating that intrathecal administration of selective CaCC inhibitors causes antiallodynic and antihyperalgesic effects in spinal nerve injured rats (Pineda-Farias et al., 2015). Similarly, knockdown of TMEM16A using siRNA (Cho et al., 2012) or ablation of TMEM16A (Lee et al., 2014) reduced acute thermal and inflammatory pain. Taken together, TMEM16A expression is required for inflammatory (Cho et al., 2012; Garcia et al., 2014) and neuropathic (this study) pain in rats.

Furthermore, immunofluorescence results indicated that TMEM16A was located in the cytoplasm and cell membranes of DRG neurons. Evidence has suggested that nociceptive neuronal TMEM16A localizes within lipid rafts of the plasma membrane and is directly coupled with IP3 receptor complexes, which allows it to be preferentially activated by Ca^{2+} released through the IP3 receptor, thus protecting TMEM16A from promiscuous activation by Ca^{2+} influx through VGCCs (Jin et al., 2013). Our previous study found that as CCI progresses, IP3 levels followed the same trend as PAR2 and TMEM16A. We speculated that increased expression of PAR2 protein caused in-creased release of IP3, leading to TMEM16A activa-tion (Zhang et al., 2018). Recent studies have also shown that activation of PAR2 increases Ca^{2+} con-centration by releasing IP3 (Huang et al., 2012). Indeed, TMEM16A acts as a heat sensor (activation threshold ~44°C), and this increase in intracellular Ca^{2+} concentration reduces the temperature threshold for TMEM16A activation. Heat-induced activation of TMEM16A depolarized DRG neurons, resulting in the generation of nociceptive signals and pain (Cho et al., 2012).

Aside from the antiallodynic effect of T16Ainh-A01, we found that this inhibitor partially diminished the CCI-induced rise in resting potential and action potential frequency of DRG neurons, and simultaneously eliminated the CCI-induced decline in action potential rheobase. This result agrees with previous observations showing that TMEM16A enhances excitability and contributes to depolarization of DRG neurons during inflammation or nerve damage (Cho et al., 2012; Lee et al., 2014). These data indicate that CCI increases the excitability of DRG neurons, and that this is partially mediated by TMEM16A activity. These findings also suggest that TMEM16A is an important molecular component contributing to peripheral pain transduction in sensory neurons.

The underlying mechanism of how nerve injury activates TMEM16A is unclear. However, nerve damage is known to cause peripheral sensitization, which leads to massive activation of excitatory mechanisms, thereby increasing intracellular Ca^{2+} levels (Latremoliere and Woolf, 2009). This response is sufficient to activate TMEM16A, which produces chloride efflux and inward currents mediating membrane potential depolarization and hyperexcitability. Thus, action potentials and pain triggered by activation of sensory neuronal TMEM16A channels and other receptors are amplified in CCI-induced conditions.

In conclusion, TMEM16A protein expression in DRG neurons was up-regulated after CCI, and the selective TMEM16A inhibitor T16Ainh-A01 reversed this increase. Furthermore, CCI increased the resting potential and action potential frequency and decreased action potential rheobase, whereas selective CaCCs inhibitor diminished this response. These results strongly suggest that TMEM16A within CaCCs that are localized to the DRG of the primary afferent neurons participate in the maintenance of neuropathic pain. However, the specific mechanism through which TMEM16A is activated after CCI and how TMEM16A participates in the generation and development of neuropathic pain remains unknown. Nevertheless, we can confirm that TMEM16A plays an important role in neuropathic pain. Preclinical studies should now comprehensively evaluate TMEM16A as a potential analgesic target

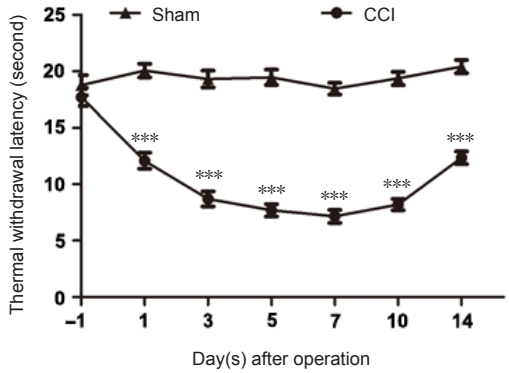

Figure 2 Pain sensitivity is determined by measuring thermal withdrawal latency on the day before and on the days after CCI.
Data are expressed as the mean ± SEM (n = 6 per group). ***P < 0.001, *vs.* sham-operated group (Student's t-test). CCI: Chronic constriction injury.

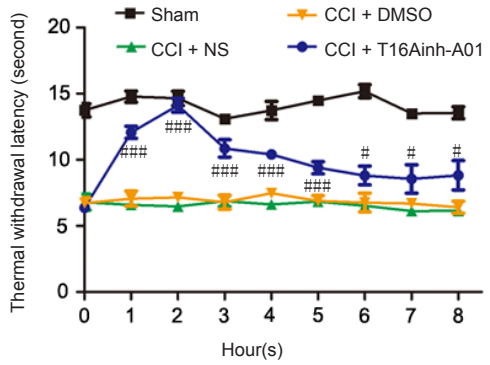

Figure 4 Intrathecal injection of the selective TMEM16A inhibitor T16Ainh-A01 attenuates CCI-induced hyperalgesia.
Time course of the antiallodynic effect of T16Ainh-A01 (10 μg) in rats subjected to CCI. Withdrawal threshold was assessed 14 days after CCI. Data are expressed as the mean ± SEM (n = 6 per group). #P < 0.05, ###P < 0.001, *vs.* CCI + DMSO group (one-way analysis of variance followed by the Student-Newman-Keuls test). CCI: Chronic constriction injury; DMSO: dimethyl sulfoxide; NS: normal saline.

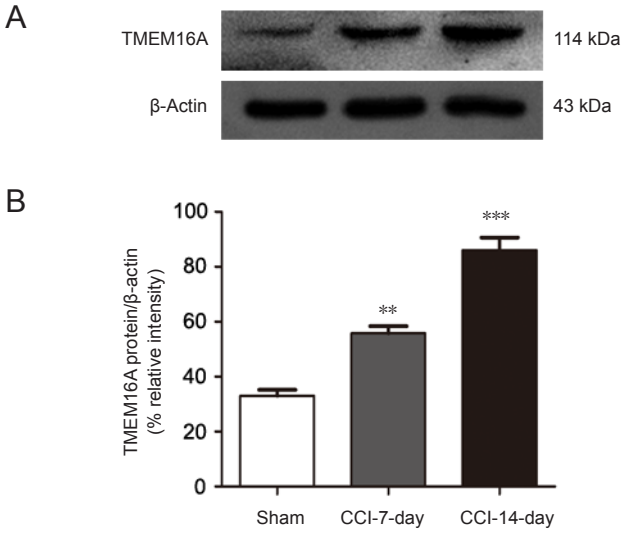

Figure 3 Expression of TMEM16A is higher in the dorsal root ganglion after CCI.
(A) Western blot images of TMEM16A expression. The upper panel shows the target band (TMEM16A protein) and the lower panel shows the loading control (beta-actin). (B) Relative level of TMEM16A protein expression. Data are expressed as the mean ± SEM (n = 6 per group). **P < 0.01, ***P < 0.001, *vs.* sham-operated group (one-way analysis of variance followed by the Student-Newman-Keuls test). CCI: Chronic constriction injury.

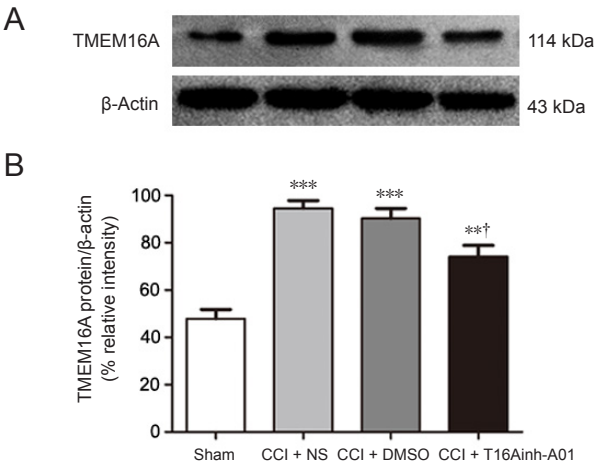

Figure 5 T16Ainh-A01 inhibits the CCI-induced activation of TMEM16A in the dorsal root ganglion of rats at 14 days after surgery.
(A) Western blot image of TMEM16A expression. The top panel shows the target band (TMEM16A protein) and the bottom one shows the loading control (beta-actin). (B) Relative level of TMEM16A protein expression. Data are expressed as the mean ± SEM (n = 6 per group). **P < 0.01, ***P < 0.001, *vs.* sham-operated group; †P < 0.05, *vs.* CCI + DMSO group (one-way analysis of variance followed by the Student-Newman-Keuls test). CCI: Chronic constriction injury; DMSO: dimethyl sulfoxide; NS: normal saline.

and determine its peripheral mechanism of action and its potential for preventing chronic pain measures in other standardized models.

Author contributions: *Study conception and design: JQS, LL and KTM; experimental data analysis and explanation: YW; implementation of the study and writing of the manuscript: QYC and CYT. All authors approved the final version of the paper.*
Conflicts of interest: *The authors declare that they have no competing interests.*
Financial support: *This study was supported by the National Natural Science Foundation of China, No. 30160026 (to JQS); the High Level Talent Research Project of Shihezi University, China, No. RCSX201705 (to YW). The funding sources had no role in study design, conception, analysis or interpretation of data, writing and deciding to submit this paper for publication.*
Institutional review board statement: *The experimental protocol was approved by the Animal Ethics Committee of First Affiliated Hospital of Shihezi University School of Medicine, China on February 27, 2017 (approval No. A2017-170-01).*

Data sharing statement: *Datasets analyzed during the current study are available from the corresponding author on reasonable request.*
Plagiarism check: *Checked twice by iThenticate.*

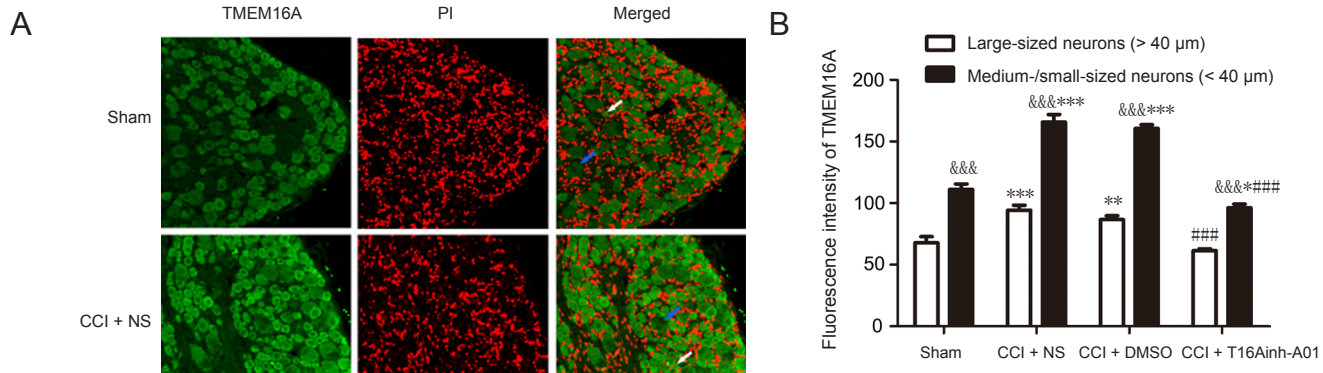

Figure 6 Expression and distribution of TMEM16A in the dorsal root ganglion of rats at 14 days after surgery (immunofluorescence).
(A) Representative images of TMEM16A immunofluorescence in dorsal root ganglion neurons in the sham and CCI + NS, CCI + DMSO, and CCI + T16Ainh-A01 groups. Scale bar: 50 μm. (B) The fluorescence intensity of TMEM16A in dorsal root ganglion neurons. **P* < 0.05, ***P* < 0.01, ****P* < 0.001, *vs.* sham-operated group; ###*P* < 0.001, *vs.* CCI + DMSO group; &&&*P* < 0.001, *vs.* large-sized dorsal root ganglion neurons (one-way analysis of variance followed by the Student-Newman-Keuls test). Blue arrows indicate representative large-sized neurons; white arrows indicate representative medium/small-sized neurons. CCI: Chronic constriction injury; DMSO: dimethyl sulfoxide; NS: normal saline; PI: propidium iodide.

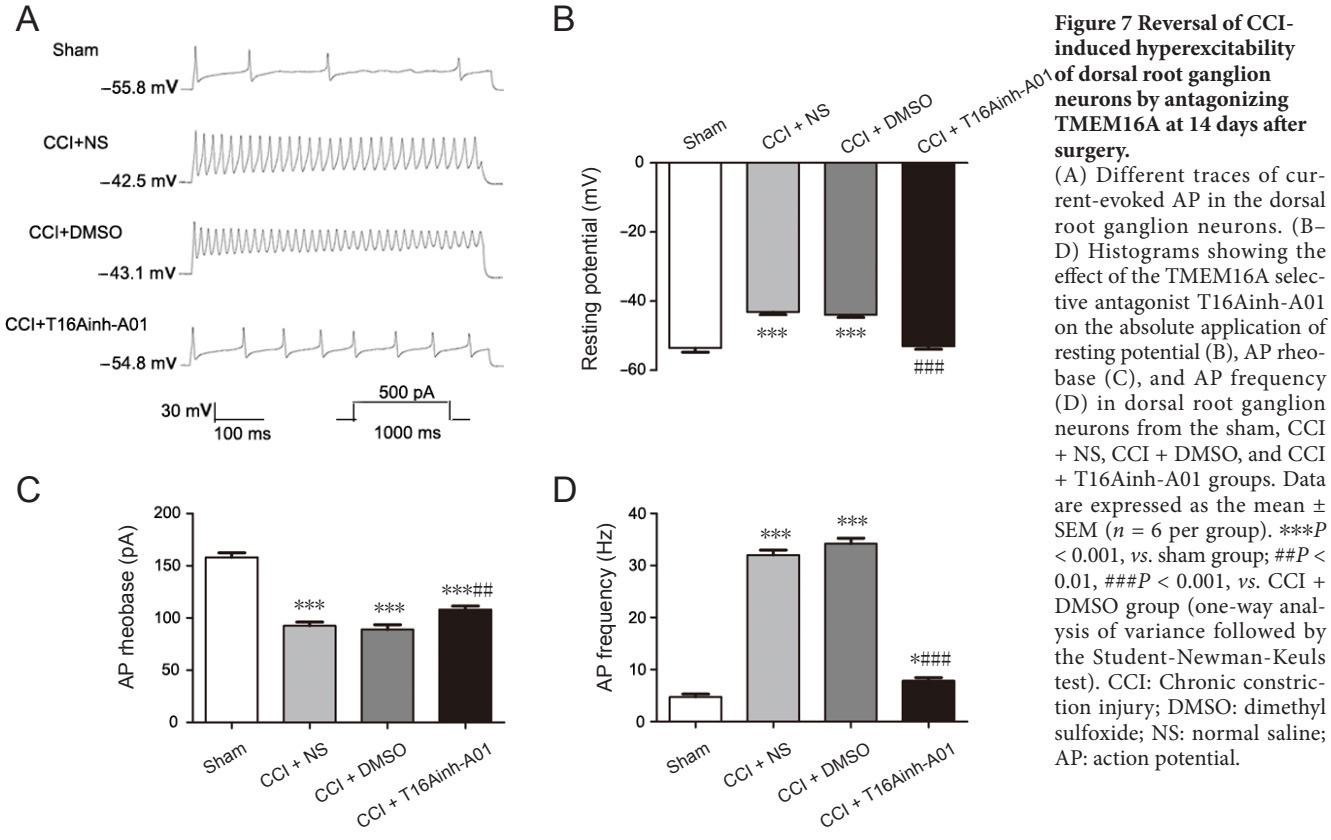

Figure 7 Reversal of CCI-induced hyperexcitability of dorsal root ganglion neurons by antagonizing TMEM16A at 14 days after surgery.
(A) Different traces of current-evoked AP in the dorsal root ganglion neurons. (B–D) Histograms showing the effect of the TMEM16A selective antagonist T16Ainh-A01 on the absolute application of resting potential (B), AP rheobase (C), and AP frequency (D) in dorsal root ganglion neurons from the sham, CCI + NS, CCI + DMSO, and CCI + T16Ainh-A01 groups. Data are expressed as the mean ± SEM (*n* = 6 per group). ****P* < 0.001, *vs.* sham group; ##*P* < 0.01, ###*P* < 0.001, *vs.* CCI + DMSO group (one-way analysis of variance followed by the Student-Newman-Keuls test). CCI: Chronic constriction injury; DMSO: dimethyl sulfoxide; NS: normal saline; AP: action potential.

Peer review: *Externally peer reviewed.*

Open peer reviewer: *Jianxun Ding, Changchun Institute of Applied Chemistry, Chinese Academy of Sciences, China.*
Additional file: *Open peer review report 1.*

References

Bennett GJ, Xie YK (1988) A peripheral mononeuropathy in rat that produces disorders of pain sensation like those seen in man. Pain 33:87-107.

Boudes M, Sar C, Menigoz A, Hilaire C, Pequignot MO, Kozlenkov A, Marmorstein A, Carroll P, Valmier J, Scamps F (2009) Best1 is a gene regulated by nerve injury and required for Ca2+-activated Cl- current expression in axotomized sensory neurons. J Neurosci 29:10063-10071.

Campbell JN, Meyer RA (2006) Mechanisms of neuropathic pain. Neuron 52:77-92.

Caputo A, Caci E, Ferrera L, Pedemonte N, Barsanti C, Sondo E, Pfeffer U, Ravazzolo R, Zegarra-Moran O, Galietta LJ (2008) TMEM16A, a membrane protein associated with calcium-dependent chloride channel activity. Science 322:590-594.

Cho H, Yang YD, Lee J, Lee B, Kim T, Jang Y, Back SK, Na HS, Harfe BD, Wang F, Raouf R, Wood JN, Oh U (2012) The calcium-activated chloride channel anoctamin 1 acts as a heat sensor in nociceptive neurons. Nat Neurosci 15:1015-1021.

Deba F, Bessac BF (2015) Anoctamin-1 Cl(-) channels in nociception: activation by an N-aroylaminothiazole and capsaicin and inhibition by T16A[inh]-A01. Mol Pain 11:55.

Deng C, Gu YJ, Zhang H, Zhang J (2017) Estrogen affects neuropathic pain through upregulating N-methyl-D-aspartate acid receptor 1 expression in the dorsal root ganglion of rats. Neural Regen Res 12:464-469.

Expert Group of Neuropathological Pain Diagnosis and Treatment (2013) Expert consensus of neuropathological pain diagnosis and treatment. Zhongguo Tengtong Yixue Zazhi 19:705-710.

García G, Martínez-Rojas VA, Rocha-González HI, Granados-Soto V, Murbartián J (2014) Evidence for the participation of Ca2+-activated chloride channels in formalin-induced acute and chronic nociception. Brain Res 1579:35-44.

Garcia G, Martinez-Rojas VA, Rocha-Gonzalez HI, Granados-Soto V, Murbartian J (2014) Evidence for the participation of Ca(2+)-activated chloride channels in formalin-induced acute and chronic nociception. Brain Res 1579:35-44.

Haanpää M, Attal N, Backonja M, Baron R, Bennett M, Bouhassira D, Cruccu G, Hansson P, Haythornthwaite JA, Iannetti GD, Jensen TS, Kauppila T, Nurmikko TJ, Rice AS, Rowbotham M, Serra J, Sommer C, Smith BH, Treede RD (2011) NeuPSIG guidelines on neuropathic pain assessment. Pain 152:14-27.

Huang ZJ, Li HC, Cowan AA, Liu S, Zhang YK, Song XJ (2012) Chronic compression or acute dissociation of dorsal root ganglion induces cAMP-dependent neuronal hyperexcitability through activation of PAR2. Pain 153:1426-1437.

Jiang R, Taly A, Grutter T (2013) Moving through the gate in ATP-activated P2X receptors. Trends Biochem Sci 38:20-29.

Jin X, Shah S, Liu Y, Zhang H, Lees M, Fu Z, Lippiat JD, Beech DJ, Sivaprasadarao A, Baldwin SA, Zhang H, Gamper N (2013) Activation of the Cl- channel ANO1 by localized calcium signals in nociceptive sensory neurons requires coupling with the IP3 receptor. Sci Signal 6:ra73.

Kang JW, Lee YH, Kang MJ, Lee HJ, Oh R, Min HJ, Namkung W, Choi JY, Lee SN, Kim CH, Yoon JH, Cho HJ (2017) Synergistic mucus secretion by histamine and IL-4 through TMEM16A in airway epithelium. Am J Physiol Lung Cell Mol Physiol 313:L466-476.

Latremoliere A, Woolf CJ (2009) Central sensitization: a generator of pain hypersensitivity by central neural plasticity. J Pain 10:895-926.

Lee B, Cho H, Jung J, Yang YD, Yang DJ, Oh U (2014) Anoctamin 1 contributes to inflammatory and nerve-injury induced hypersensitivity. Mol Pain 10:5.

Li Y, Feng C, Ning M, Xu F, Song ZH, Guang ZB, Xiao HY (2018) Angiotensin II receptor antagonist EMA401 used for sciatic nerve constriction-induced neuropathic pain in rats: behavior assessment and anaIgesic mechanisms. Zhongguo Zuzhi Gongcheng Yanjiu 22:1909-1914.

Olukman M, Önal A, Celenk FG, Uyanıkgil Y, Cavuşoğlu T, Düzenli N, Ülker S (2018) Treatment with NADPH oxidase inhibitor apocynin alleviates diabetic neuropathic pain in rats. Neural Regen Res 13:1657-1664.

Pineda-Farias JB, Barragán-Iglesias P, Loeza-Alcocer E, Torres-López JE, Rocha-González HI, Pérez-Severiano F, Delgado-Lezama R, Granados-Soto V (2015) Role of anoctamin-1 and bestrophin-1 in spinal nerve ligation-induced neuropathic pain in rats. Mol Pain 11:41.

Pogatzki EM, Zahn PK, Brennan TJ (2000) Lumbar catheterization of the subarachnoid space with a 32-gauge polyurethane catheter in the rat. Eur J Pain 4:111-113.

Ruppersburg CC, Hartzell HC (2014) The Ca2+-activated Cl- channel ANO1/TMEM16A regulates primary ciliogenesis. Mol Biol Cell 25:1793-1807.

Schroeder BC, Cheng T, Jan YN, Jan LY (2008) Expression cloning of TMEM16A as a calcium-activated chloride channel subunit. Cell 134:1019-1029.

Tölle TR (2010) Challenges with current treatment of neuropathic pain. Eur J Pain Suppl 4:161-165.

Wang LJ, Wang Y, Chen MJ, Tian ZP, Lu BH, Mao KT, Zhang L, Zhao L, Shan LY, Li L, Si JQ (2017) Effects of niflumic acid on gamma-aminobutyric acid-induced currents in isolated dorsal root ganglion neurons of neuropathic pain rats. Exp Ther Med 14:1373-1380.

Wang Q, Leo MD, Narayanan D, Kuruvilla KP, Jaggar JH (2016) Local coupling of TRPC6 to ANO1/TMEM16A channels in smooth muscle cells amplifies vasoconstriction in cerebral arteries. Am J Physiol Cell Physiol 310:C1001-1009.

Wu MM, Lou J, Song BL, Gong YF, Li YC, Yu CJ, Wang QS, Ma TX, Ma K, Hartzell HC, Duan DD, Zhao D, Zhang ZR (2014) Hypoxia augments the calcium-activated chloride current carried by anoctamin-1 in cardiac vascular endothelial cells of neonatal mice. Br J Pharmacol 171:3680-3692.

Xiao Y, Wu Y, Zhao B, Xia Z (2016) Decreased voltage-gated potassium currents in rat dorsal root ganglion neurons after chronic constriction injury. Neuroreport 27:104-109.

Yamamura H, Nishimura K, Hagihara Y, Suzuki Y, Imaizumi Y (2018) TMEM16A and TMEM16B channel proteins generate Ca2+-activated Cl- current and regulate melatonin secretion in rat pineal glands. J Biol Chem 293:995-1006.

Yang J, Xie MX, Hu L, Wang XF, Mai JZ, Li YY, Wu N, Zhang C, Li J, Pang RP, Liu XG (2018) Upregulation of N-type calcium channels in the soma of uninjured dorsal root ganglion neurons contributes to neuropathic pain by increasing neuronal excitability following peripheral nerve injury. Brain Behav Immun 71:52-65.

Yang YD, Cho H, Koo JY, Tak MH, Cho Y, Shim WS, Park SP, Lee J, Lee B, Kim BM, Raouf R, Shin YK, Oh U (2008) TMEM16A confers receptor-activated calcium-dependent chloride conductance. Nature 455:1210-1215.

Yoon JH, Son JY, Kim MJ, Kang SH, Ju JS, Bae YC, Ahn DK (2018) Preemptive application of QX-314 attenuates trigeminal neuropathic mechanical allodynia in rats. Korean J Physiol Pharmacol 22:331-341.

Zhang M, Gao CX, Wang YP, Ma KT, Li L, Yin JW, Dai ZG, Wang S, Si JQ (2018) The association between the expression of PAR2 and TMEM16A and neuropathic pain. Mol Med Rep 17:3744-3750.

Zimmermann M (1983) Ethical guidelines for investigations of experimental pain in conscious animals. Pain 16:109-110.

P-Reviewer: Ding J; C-Editor: Zhao M; S-Editors: Yu J, Li CH; L-Editors: Phillips A, Qiu Y, Song LP; T-Editor: Liu XL